Adaptation and parametrization of an iron loss model for rotating magnetization loci in NO electrical steel

Benedikt Schauerte, Martin Marco Nell, Tim Brimmers, Nora Leuning and Kay Hameyer
Institute of Electrical Machines (IEM), Rheinisch Westfalische Technische Hochschule Aachen University, Aachen, Germany

Received 28 June 2021
Revised 8 September 2021
Accepted 21 September 2021

Abstract

Purpose – The magnetic characterization of electrical steel is typically examined by measurements under the condition of unidirectional sinusoidal flux density at different magnetization frequencies. A variety of iron loss models were developed and parametrized for these standardized unidirectional iron loss measurements. In the magnetic cross section of rotating electrical machines, the spatial magnetic flux density loci and with them the resulting iron losses vary significantly from these unidirectional cases. For a better recreation of the measured behavior extended iron loss models that consider the effects of rotational magnetization have to be developed and compared to the measured material behavior. The aim of this study is the adaptation, parametrization and validation of an iron loss model considering the spatial flux density loci is presented and validated with measurements of circular and elliptical magnetizations.

Design/methodology/approach – The proposed iron loss model allows the calculation and separation of the different iron loss components based on the measured iron loss for different spatial magnetization loci. The separation is performed in analogy to the conventional iron loss calculation approach designed for the recreation of the iron losses measured under unidirectional, one-dimensional measurements. The phenomenological behavior for rotating magnetization loci is considered by the formulation of the different iron loss components as a function of the maximum magnetic flux density B_m, axis ratio f_{Ax}, angle to the rolling direction (RD) θ and magnetization frequency f.

Findings – The proposed formulation for the calculation of rotating iron loss is able to recreate the complicated interdependencies between the different iron loss components and the respective spatial magnetic flux loci. The model can be easily implemented in the finite element analysis of rotating electrical machines, leading to good agreement between the theoretically expected behavior and the actual output of the iron loss calculation at different geometric locations in the magnetic cross section of rotating electrical machines.

Originality/value – Based on conventional one-dimensional iron loss separation approaches and previously performed extensions for rotational magnetization, the terms for the consideration of vectorial unidirectional, elliptical and circular flux density loci are adjusted and compared to the performed rotational measurement. The presented approach for the mathematical formulation of the iron loss model also allows the parametrization of the different iron loss components by unidirectional measurements performed in different directions to the RD on conventional one-dimensional measurement topologies such as the Epstein frames and single sheet testers.

Keywords Magnetic hysteresis, Iron losses, Soft magnetic materials, Rotational magnetization, Iron loss separation, Vector hysteresis, Electrical steel

Paper type Research paper

This work was supported by the Deutsche Forschungsgemeinschaft (DFG) in the DFG priority program "SPP2013 – Focused Local Stress Imprint in Electrical Steel as Means of Improving the Energy Efficiency"-HA 4395/22-1 and in the DFG research group project "FOR 1897 – Low-Loss Electrical Steel for Energy-Efficient Electrical Drives" and as part of the DFG research project "Improved modeling and characterization of ferromagnetic materials and their losses."

COMPEL – The international journal for computation and mathematics in electrical and electronic engineering
Vol. 41 No. 2, 2022
pp. 589-599

0332-1649
DOI 10.1108/COMPEL-06-2021-0218

1. Introduction

The accurate calculation of the resulting iron loss distribution in the post-processing of the numerical simulation of electrical machines is crucial for the design and development of electrical drives. Standardized iron loss measurements are primarily performed under sinusoidal unidirectional waveforms of the magnetic flux density at different flux densities B_m and magnetization frequencies f. The measurements performed under these conditions only recreate the actual course of the magnetic flux density and the resulting losses in the magnetic circuit of rotating electrical machines to a very limited extent as depicted in Figure 1. Rotational single sheet testers (RSST) were developed to characterize the resulting iron losses under the influence of rotating magnetization (Müller *et al.*, 2019; Zurek and Meydan, 2006). These magnetic sensors allow the vector characterization of the material under the influence of varying *locus* curves in the sheet metal plane. The iron losses measured under these conditions differ from the material behavior measured under one-dimensional conditions and cannot be mapped with sufficient accuracy using conventional iron loss models, which were formulated and parameterized on the basis of one-dimensional measurements (Enokizono *et al.*, 1991).

In Figure 1, three resulting exemplarily *locus* curves of an finite element-simulation of an induction machine are depicted. While the magnetic flux loci in the middle of the stator teeth corresponds strongly to the typically evaluated unidirectional waveforms, the *locus* curves at the origin and the transition region show approximately circular and elliptical courses. The simulated flux density loci can be approximated by unidirectional, elliptical and circular courses and mathematically described by the maximum magnetic excitation B_m, the axis ratio f_{Ax} and the displacement angle to the rolling direction (RD) θ as depicted in Figure 2. The parameter f_{Ax} represents the width of the ellipse and is derived from the quotient of the minimum flux density B_{min} in the transverse direction to the maximum magnetic flux density in the main direction B_{max} of the ellipsoid. To ensure a continuity of the notation of previous loss models, the *locus* curves are represented by B_m and f_{Ax}.

As confirmed by many studies, the resulting iron loss and its components are influenced in different ways and by the respective *locus* curves. For rotating magnetizations, there is initially an increase in the resulting iron losses of up to 2.5 times the unidirectional measurements in the range of lower magnetic flux densities. This effect occurs because of the increased domain wall movements in the unsaturated measuring range and the increased eddy currents because of the additional induced voltage. In the area of increased magnetizations up to saturation this effect is reversed, as the magnetic moments overcome

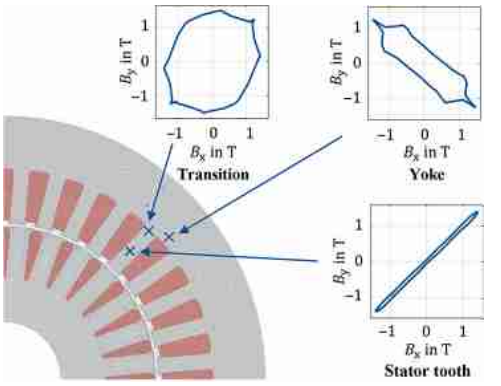

Figure 1.
Different simulated locus curves of the magnetic flux density as a function of the considered geometrical position in the magnetic cross section of an induction machine

the magnetic anisotropy with a certain magnetic excitation and start to rotate, following the applied magnetic field strength. As a consequence, the movement of the magnetic domain walls strongly reduces, leading to a significant decline of the hysteresis and excess loss components (Appino *et al.*, 2016).

To consider the different simulated flux density loci, extended iron loss models are required that recreate the complex behavior of the iron losses P_{Fe} as a function of the three mentioned parameters describing the shape of the approximated loci and the magnetization frequency f. In this paper, a unidirectional iron loss formulation based on a loss separation approach is expanded and parametrized to recreate the iron loss behavior under the influence of rotational magnetizations.

2. Rotational iron loss measurements

The waveform of the respective *locus* of the magnetic flux density is determined by the maximum excitation B_m, the axis ratio f_{Ax} and the angle θ between the main axis of the ellipsoid and the RD as depicted in Figure 2. The measurements are carried out with a RSST, which is described thoroughly in Thul *et al.* (2018). The magnetic flux density is measured by two vertically arranged B-coils brought into the sample through two bore holes for each direction. The diameter of the circuit drill was chosen relatively small of 0.4 mm to reduce the influence on the magnetic properties of the sample. The local magnetic field strength is measured by four H-coils placed very closely in precisely defined distances to the sample surface. The two H-coils used for each direction (RD and Transverse direction (TD) also referred as x- and y-direction) enable the approximation of the local magnetic field strength $\vec{H}$ on the surface of the sample. The magnetization of the sample in the two main directions is applied by two magnetization windings in each of the yoke legs, which are arranged in a cross shape toward the sample in the middle of the topology. The measurements can be performed at magnetization frequencies between 50 and 1000 Hz at maximum magnetic flux densities B_m of 1.5 T. The axis ratio f_{Ax} and the angle θ to the RD can be chosen arbitrary. For each measured combination of f, B_m, f_{Ax} and θ, the measurements are carried out clockwise (cw) and counter clockwise (ccw) to erase parasitic effects by averaging the measured iron loss of both the rotational directions as described in Mori *et al.* (2011) and Maeda *et al.* (2008). A comparison of the rotating iron losses measured in different directions of rotation and the averaged curve is shown in Figure 3.

The special cases of the loci of unidirectional ($f_{Ax} = 0$) and circular courses of the magnetic flux density ($f_{Ax} = 1$) are of particular importance for the characterization of the iron loss behavior. Nonetheless, during the operation of rotating electrical machines, a variety of combinations of elliptic shapes and inclination angles occurs depending on the

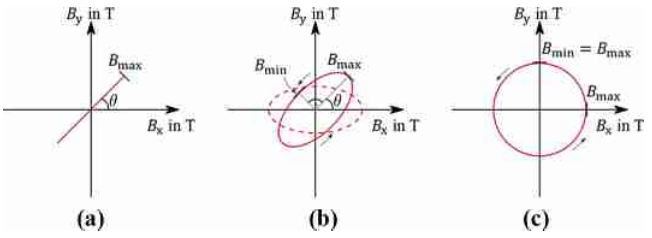

Figure 2.
Different magnetic flux density loci for a) unidirectional (f_{Ax} = 0), b) elliptical (f_{Ax} = 0.5) magnetization with the angle θ between main axis and RD and circular magnetization (f_{Ax} = 1.0) in (c)

respective operation point and location on the magnetic cross section of the machine. Thus, the transition between unidirectional and rotational magnetization must be considered in the magnetic characterization of the material as in the simulation of the iron loss components. The measurements presented and discussed in this work were carried out for three different fully processed Non-oriented (NO) electrical steel materials as shown in Table 1.

The rotational iron loss measurements depicted in Figure 4 were performed cw and ccw at 0, 45 and 90° to the RD for five axis ratios f_{Ax} at 100 Hz, with a peak flux density of up to 1.5 T for material *M*1. The measurements show the typical increase of the iron losses to more than double in the magnetization range of up to 1.0 T for circular rotating flux density

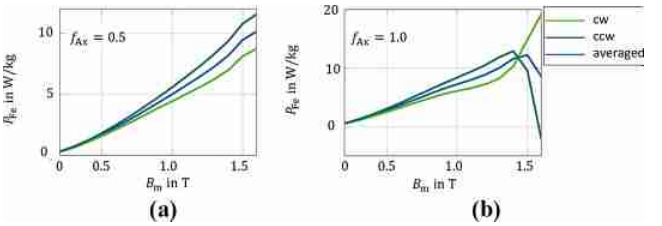

Figure 3.
Elliptical (a) and circular (b) rotational measurements performed in cw and ccw and averaged measured iron loss P_{Fe} with respect to B_m at 200 Hz

Material	Specific density ρ (kg/m^3)	Thickness (mm)	Weight (g)
*M*1	7,530	0.24	6.50
*M*2	7,650	0.26	7.11
*M*3	7,650	0.26	7.15

Table 1.
Parameters of evaluated NO electrical steel sheets

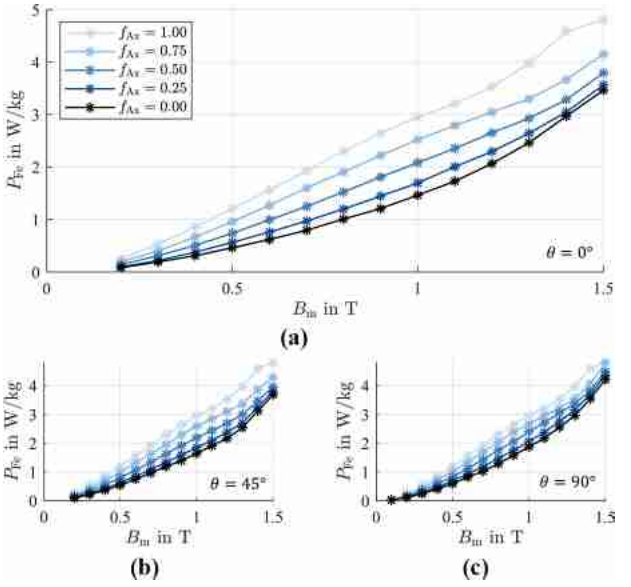

Figure 4.
Measured iron loss of *M*1 with main axis in 0°, 45° and 90° to the RD measured at increasing axis ratios f_{Ax} and 100 Hz

loci (f_{Ax} = 1.0) in comparison to unidirectional magnetization (f_{Ax} = 0). The behavior in the transition is non-linear and magnetization-dependent with regard to the losses as a function of the axis ratio. The decrease of losses in the case of circular magnetization is indicated between 1.3 and 1.5 T. Although for the circular magnetization no influence of the magnetic anisotropy occurs by principle, the unidirectional and elliptical measurements reveal the influence of the magnetic anisotropy on the resulting iron loss. Although the iron loss density for a circular magnetization of 1.0 T is 2.953 W/kg for each angle to the RD by principle, the unidirectional measurements in 0°, 45° and 90° result in 1.464, 1.646 and 1.871 W/kg, respectively. The influence of the angle to the RD declines with increasing axis ratio f_{Ax}. The large number of adjustable parameters for the measurements leads to a considerable measurement effort per material. The set operation points per material are shown in Table 2.

The measurements performed on *M*2 and *M*3 are depicted in Figure 5, which confirm the measured behavior for *M*1 with maximum ratio between circular and unidirectional measurements of 2.804 W/kg for *M*2 at 0.6 T. The difference then declines for magnetic peak flux densities higher than 1.0 T. Because of saturation effects, the measurements are limited to a maximum peak flux density of 1.5 T. The transition to lower iron losses for the circular magnetization is therefore only indicated in the measurements carried out.

The measurement results shown in Figure 6 for the three materials under consideration at magnetization frequencies of 800 Hz show that the influence of different local field loci decreases relatively slightly at higher frequencies. In absolute terms, however, it still has a considerable influence on the resulting iron losses. The complex behavior of the excess and hysteresis component, which decreases in its significance on the total losses at higher frequencies, is now offset by strongly increased eddy current loss components. The transition to decreasing iron loss proportions of P_{hyst} and P_{exc} can be seen more clearly in the high-frequency measurements, especially in the measurements performed for *M*2 and *M*3.

3. Iron loss model approach

To simulate and calculate the complex, measured material behavior of rotating electrical machines, iron loss models are required that map the material behavior as precisely as

Material	F (Hz)	B_m (T)	f_{Ax}	θ (°)
*M*1	50, 100, 200,	0.1 up to 1.6 T in	0, 0.25, 0.5, 0.75 and 1.0	0, 45 and 90
*M*2	400 and 800	steps f 0.1 T	0, 0.5 and 1.0	0 and 90
*M*3			0 and 1.0	0 and 90

Table 2. Measurement points for vectorial characterization of examined materials

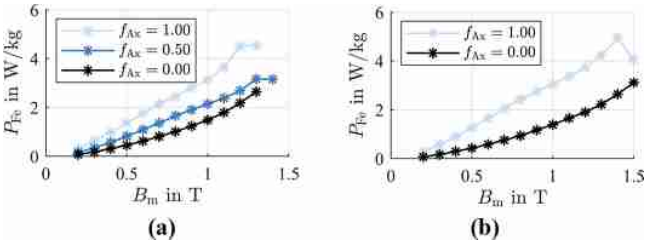

Figure 5. Measured iron loss for a) *M*2 and b) *M*3 for θ = 0° at 100 Hz

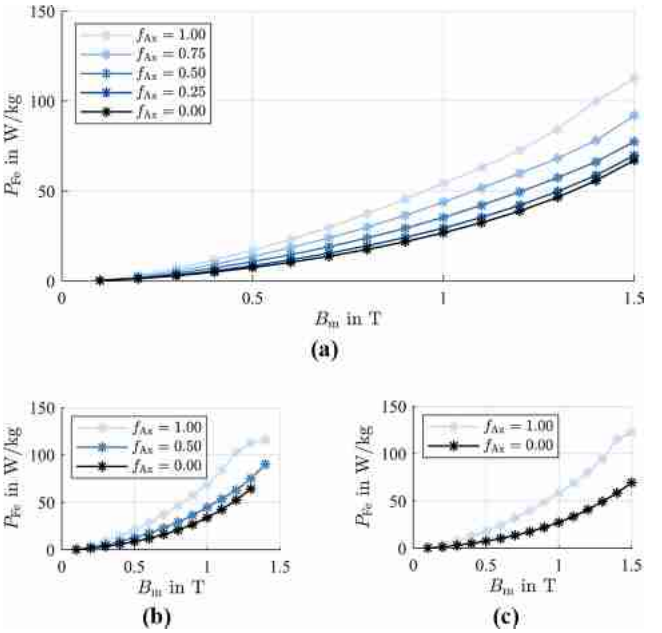

Figure 6.
Measured iron loss for increasing axis ratios for a) $M1$, b) $M2$ and c) $M3$. Magnetization frequency at 800 Hz with $\theta = 0°$

possible with regard to the input parameters. The basis of the extended iron loss formulation is the unidirectional separation approach in Eggers *et al.* (2012):

$$P_{\mathrm{Fe}}\ P_{\mathrm{hyst}} + P_{\mathrm{cl}} + P_{\mathrm{exc}} + P_{\mathrm{sat}} \tag{1}$$

Based on the unidirectional IEM formulation for consideration of saturation effects and field displacement at magnetization frequencies over 400 Hz and magnetic flux densities higher than 1.5 T, an approach for the consideration of the effects of rotational magnetization on the resulting iron losses was presented in Steentjes *et al.* (2012):

$$P_{\mathrm{hyst}} = a_1 \cdot \left(1 + f_{\mathrm{Ax}} \cdot \left(r_{\mathrm{hyst}} - 1\right)\right) \cdot B_{\mathrm{m}}^{\alpha} \cdot f \tag{2}$$

$$P_{\mathrm{cl}} = a_2 \cdot B_{\mathrm{m}}^{2} \cdot f^{2} \tag{3}$$

$$P_{\mathrm{exc}} = a_5 \cdot \left(1 + f_{\mathrm{Ax}} \cdot \left(r_{\mathrm{exc}} - 1\right)\right) \cdot B_{\mathrm{m}}^{1.5} \cdot f^{1.5} \tag{4}$$

$$P_{\mathrm{sat}} = a_2 \cdot a_3 \cdot B_{\mathrm{m}}^{a_4+2} \cdot f^{2} \tag{5}$$

The behavior of the loss components P_{hyst} and P_{exc} are considered by the additional rotational iron loss factors r_{hyst} and r_{exc}, which are interpreted as a homogeneously, piecewise linear decreasing function as depicted in Figure 7(a) based on rotational iron loss measurements from the literature (Appino *et al.*, 2009; Appino *et al.*, 2016). The transition from unidirectional to circular magnetization was only considered by the multiplication of the axis ratio f_{Ax} according to the iron loss components.

The iron loss model proposed in this work is an adaptation of the IEM iron loss separation approach presented in Schauerte *et al.* (2019). The focus is on the best possible representation of the measured iron losses as a function of B_m, f, θ and f_{Ax}. In addition to the previously considered hysteresis-, classical- and excess-loss components, the presented model is expanded by the saturation loss component P_{sat}. The components P_{cl} and P_{sat} are not influenced by the respective *locus* and are calculated from the vectorial decomposition of the flux density in B_{max} and B_{min} as follows:

$$P_{hyst} = \left(1 - f_{Ax}^2 \cdot r_{hyst}\right) B_m^{\alpha + B_m \beta} \left(a_1 + f_{Ax}^{\alpha + B_m \beta} a_{1,90°}\right) f \tag{6}$$

$$P_{cl} = a_2 \cdot B_m^2 \cdot \left(1 + f_{Ax}^2\right) \cdot f^2 \tag{7}$$

$$P_{exc} = \left(1 - f_{Ax}^2 \cdot r_{exc}\right) \cdot B_m^{1.5} \cdot \left(a_5 + f_{Ax}^{1.5} \cdot a_{5,90°}\right) \cdot f^{1.5} \tag{8}$$

$$P_{sat} = a_2 \cdot a_3 \cdot B_m^{a_4+2} \cdot \left(1 + f_{Ax}^{a_4+2}\right) \cdot f^2 \tag{9}$$

The complicated behavior of the hysteresis and excess loss components with regard to the peak polarization and the *locus* curve of the magnetic flux density is considered by the squared axis ratio and the additional factor r_{hyst} respective r_{exc}. Although both loss mechanisms are based on domain wall movements, the dependencies to peak magnetization and axis ratio differs as presented in Appino *et al.* (2016). As a distinction between these two influences can only be performed by quasi-static measurements, for the time being both components are set equal to the following:

$$r_{hyst,exc} = J_m \cdot \frac{P_{Fe}(J_m)}{J_s \cdot P_{Fe,S}} \tag{10}$$

The iron loss characteristic for the calculation of r_{hyst} and r_{exc} in equation (6) are identified by averaging unidirectional measurements in different directions to RD to consider the iron loss behavior within the entire sheet plane and not just one single direction. Another advantage of the proposed formulation is that all model parameters can also be identified by unidirectional measurements on a conventional Epstein frame or single sheet testers (SST). J_s denotes the saturation polarization of the respective material, whereas J_m denotes the peak polarization of the actual *locus* curve. $P_{Fe}(J_m)$ represents the measured iron loss averaged across all-measured inclination angles and frequencies of unidirectional measurements. P_{Fe} stands for the losses extrapolated to the saturation polarization. Unlike the curve shown on the left in Figure 7(a) for the parameters r_{hyst} and r_{exc}, which are assumed on empirical analysis of typical rotating

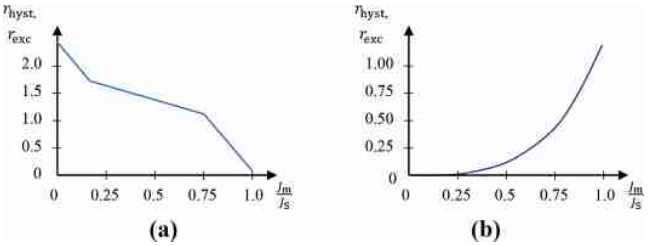

Figure 7.
Original rotational loss factors r_{hyst} and r_{exc} (left) and adapted version based on measurements (right) as a function of saturation state of material

measurements regardless of the material, the curve shown in Figure 7(b) of the losses and can be determined for each material using one-dimensional SST measurements (Figure 8).

A depiction of the actual progression of the individual iron loss components, the calculated iron loss proportions are plotted as a function of the maximum magnetic flux density B_m and the axial ratio f_{Ax} for a magnetization frequency of 50 Hz. The classical eddy current loss component P_{cl} increases monotonously with for both variables, whereas the saturation component P_{sat} only depends on the maximum peak flux density B_m. The hysteresis and excess loss components however are strongly influenced by both quantities, resulting in an increase of both components for small values of B_m, whereas the transition to decreasing losses takes place for increasing rotational magnetizations. To allow the examination of the resulting iron losses at magnetization angles that have not been specifically measured, a linear transition between the identified parameters can be performed to approximate the angles θ in between the angles measured.

4. Simulation of iron loss

Based on the unidirectional measurements performed on the three examined materials, the iron loss parameters for the proposed model were identified for the RD and TD. The resulting parameters are depicted in Table 3. The rotational iron loss factors r_{hyst} and r_{exc} were calculated according to equation (10).

The simulation results depicted in Figure 9 show the good accordance between measurement and simulation for a wide frequency range and for all axis ratios, especially the transition from unidirectional to circular magnetization for magnetic flux densities B_m below 1.3 T. When comparing measurement and simulation at 50 Hz, it is noticeable that the simulation overestimates the unidirectional losses, whereas the iron loss for elliptical and circular magnetization are underestimated in the range of smaller magnetizations. Generally, the accordance between measurement and simulation increases in its accuracy with increasing magnetization frequencies f. It can be assumed that with additional performed measurements at quasi-static frequencies could furtherly improve the model's accuracy at low frequencies. Nonetheless, the phenomenological behavior of the iron losses is mapped qualitatively well across the entire examined range of magnetization B_m, axis ratio f_{Ax} and magnetization frequencies f.

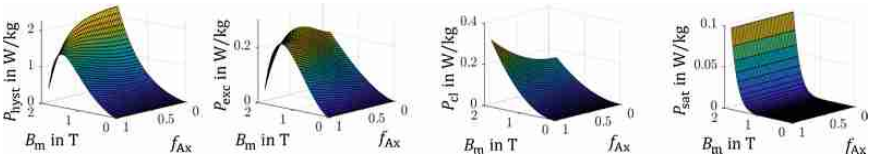

Figure 8.
Simulated iron loss components as function peak flux density B_m and the axis ratio f_{Ax} for a magnetization frequency of 50 Hz

Table 3.
Iron loss parameters identified by unidirectional measurements of examined NO materials

Material	a_1	a_2	a_3	a_4	a_5	$a_{1,90°}$	$a_{5,90°}$	α	β
*M*1	0.01	$2.1355 \cdot 10^{-5}$	0.005837	7.8138	0.0002	0.01202	0.0003	1.5235	0.5649
*M*2	0.0056145	$3.4096 \cdot 10^{-05}$	0.023854	4.7701	0.00062442	0.0084217	0.00093663	1.7468	0.33834
*M*3	0.0087046	$2.2136 \cdot 10^{-5}$	0.026598	4.199	0.0003588	0.013057	0.00038646	1.6533	0.11909

The comparison between measurement and simulation with additional decomposition of the individual loss components is presented in Figure 10. The measured behavior is again met with satisfactory accordance across the entire scope of measurement parameters. The comparison of the different compositions of iron loss components confirms the behavior that can be expected based on the theory of iron loss for rotational magnetizations. Compared to the conventional distribution of the loss components for an axis ratio of 0, the hysteresis and excess components increase across the entire measurement range for $f_{Ax} = 0.5$. The eddy current losses P_{cl} also increase with the increasing additional vector component. For circular magnetization, the typical drop in hysteresis and excess components occurs with high magnetization after initial growth in the area of low magnetizations. The eddy current losses P_{cl} keep increasing with the axis ratio and respective peak flux density B_m. As mentioned in description of the loss formulation approach, the saturation loss component for the time being only depends on the respective peak flux density and thus behaves constant for each examined axis ratio f_{Ax}. Despite the generally good agreement between measurements and simulation, it must be emphasized that the simulated behavior above 1.5 T is an extrapolation of the expected material behavior. The simulated loss behavior in the saturated range represents an extrapolation of the measurement data based on the behavior presented in the literature.

Exemplary results for the also examined materials $M2$ and $M3$ are depicted in Figure 11 and Figure 12, respectively. As for material $M1$, the iron loss parameters were also

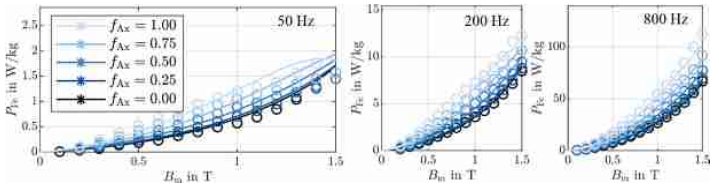

Figure 9.
Measured (dots) and simulated (solid lines) iron losses for increasing axis ratios f_{Ax} at 50, 200 and 800 Hz with $\theta = 0°$ for $M1$

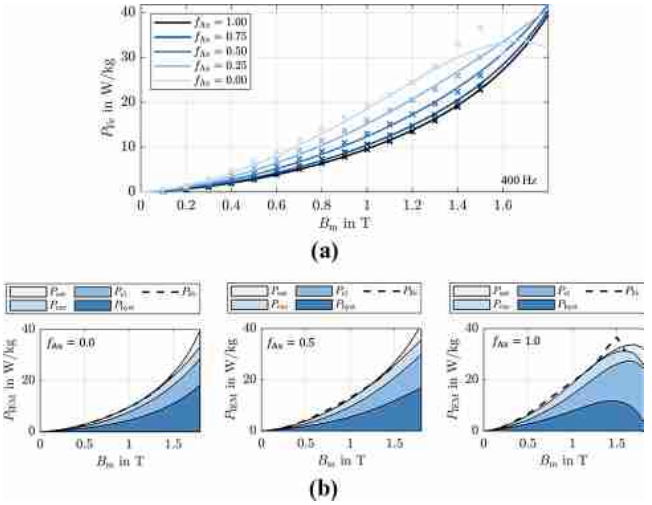

Figure 10.
Measured (crosses) and simulated (solid lines) iron loss for increasing axis ratios f_{Ax} a) and simulated iron loss components vs measurements (dashed line) b) at 400 Hz of $M1$ for $\theta = 0°$

determined here on the basis of the unidirectional measurements at 0 and 90° to the RD of performed for materials *M*2 and *M*3. The simulation results are plotted against the measurements for main angles θ of 0 and 90°. Because of the magnetic anisotropy, the difference between the unidirectional and circular loss measurements for both materials is significantly smaller than for the unidirectional measurement in the RD. However, because of the vector structure of the iron loss formulation, this effect can be successfully mapped and considered in the simulations. Despite slight deviations occurring here and between measurement and simulation, the material behavior can be successfully simulated with respect to the examined influencing quantities.

5. Conclusions and further work

In this work rotating iron loss measurements were performed for three different NO electrical steel sheets in a magnetization frequency range from 50 to 800 Hz. The adjustable input parameters were the peak flux density B_m, magnetization frequency f, the axis ratio f_{Ax} and the offset of the main axis to the RD θ in their influences on the resulting iron losses P_{Fe}. To suppress parasitic effects, all rotating measurements were carried out cw and ccw and then averaged.

An iron loss separation approach for the consideration of rotational and elliptical loci of magnetic flux density was further developed on the basis of two existing iron loss models. To consider the magnetic anisotropy, the model can be parameterized using any number of unidirectional measurements in different spatial directions, which can also be carried out on conventional one-dimensional measurement topologies. The model presented is in good agreement with the rotating iron loss measurements carried out and successfully depicts the phenomenological behavior of the various iron loss components even in the non-measurable saturation range in accordance with the behavior known from the literature. For the future,

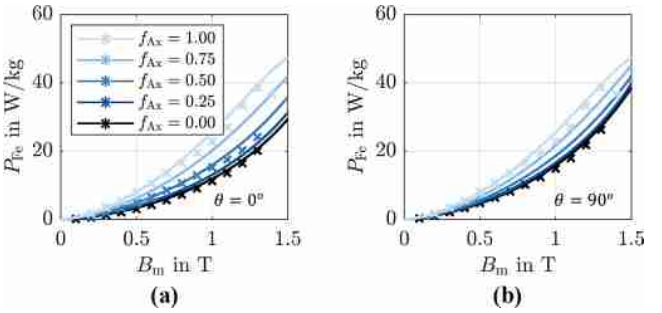

Figure 11.
Measured (crosses) and simulated (solid) lines for $f = 400$ Hz and increasing f_{Ax} for *M*2

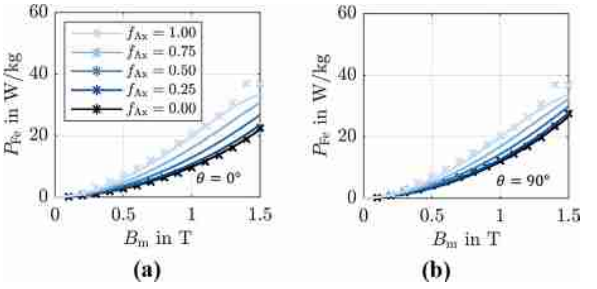

Figure 12.
Measured (crosses) and simulated (solid) lines for $f = 400$ Hz and increasing f_{Ax} for *M*3

it would be interesting to expand the measuring range to include higher magnetic flux densities and lower frequencies to further adapt the rotating iron loss parameters r_{hyst} and r_{exc}, also with regard to an individual consideration of the two effects. The implementation of the model in the post-processing of an induction machine could also be carried out successfully and is presented in Nell *et al.* (2020).

References

Appino, C., Fiorillo, F. and Ragusa, C. (2009), "One-dimensional/two-dimensional loss measurements up to high inductions", *Journal of Applied Physics*, Vol. 105 No. 7, p. 07E718.

Appino, C., Khan, M., De La Barriere, O., Ragusa, C. and Fiorillo, F. (2016), "Alternating and rotational losses up to magnetic saturation in non-oriented steel sheets", *IEEE Transactions on Magnetics*, Vol. 52 No. 5, pp. 1-4.

Eggers, D., Steentjes, S. and Hameyer, K. (2012), "Advanced iron-loss estimation for nonlinear material behavior", *IEEE Transactions on Magnetics*, Vol. 48 No. 11, pp. 3021-3024.

Enokizono, M., Suzuki, T. and Sievert, J.D. (1991), "Measurement of iron loss using rotational magnetic loss measurement apparatus", *IEEE Translation Journal on Magnetics in Japan*, Vol. 6 No. 6, pp. 508-514.

Maeda, Y., Shimoji, H., Todaka, T. and Enokizono, M. (2008), "Study of the counterclockwise/clockwise (CCW/CW) rotational losses measured with a two-dimensional vector magnetic property measurement system", *IEEJ Transactions on Electrical and Electronic Engineering*, Vol. 3 No. 2, pp. 222-228.

Mori, Y., Miyagi, D., Nakano, M. and Takahashi, N. (2011), "Measurement of magnetic properties of Grain-Oriented electrical steel sheet using 2D single sheet tester", *Przeglad Elektrotechniczny (Electrical Review)*, Vol. 87 No. 9, pp. 47-51.

Müller, F., Bavendiek, G., Schauerte, B. and Hameyer, K. (2019), "Measurement and simulation of a rotational single sheet tester", *Archives of Electrical Engineering*, Vol. 68 No. 1.

Nell, M., Schauerte, B., Brimmers, T. and Hameyer, K. (2020), "Analysis of simulated iron losses in electrical machines using different iron loss models", Manuscript submitted to EPNC 2020 for publication.

Schauerte, B., Steentjes, S., Thul, A. and Hameyer, K. (2019), "Iron-loss model for arbitrary magnetization loci in NO electrical steel", *International Journal of Applied Electromagnetics and Mechanics*, Vol. 61 No. S1, pp. 89-96.

Steentjes, S., Leßmann, M. and Hameyer, K. (2012), "Advanced iron-loss calculation as a basis for efficiency improvement of electrical machines in automotive application", *2012 Electrical Systems for Aircraft, Railway and Ship Propulsion*, *IEEE*, October, pp. 1-6.

Thul, A., Steentjes, S., Schauerte, B., Klimczyk, P., Denke, P. and Hameyer, K. (2018), "Rotating magnetizations in electrical machines: Measurements and modeling", *AIP Advances*, Vol. 8 No. 5, p. 056815.

Zurek, S. and Meydan, T. (2006), "Rotational power losses and vector loci under controlled high flux density and magnetic field in electrical steel sheets", *IEEE Transactions on Magnetics*, Vol. 42 No. 10, pp. 2815-2817.

Corresponding author
Benedikt Schauerte can be contacted at: benedikt.schauerte@iem.rwth-aachen.de